

# Sodium Flux Ratio in Na/K Pump-Channels Opened by Palytoxin

R.F. Rakowski, Pablo Artigas, Francisco Palma, Miguel Holmgren, Paul De Weer, and David C. Gadsby

Marine Biological Laboratory, Woods Hole, MA 02543

Palytoxin binds to Na<sup>+</sup>/K<sup>+</sup> pumps in the plasma membrane of animal cells and opens an electrodiffusive cation pathway through the pumps. We investigated properties of the palytoxin-opened channels by recording macroscopic and microscopic currents in cell bodies of neurons from the giant fiber lobe, and by simultaneously measuring net current and <sup>22</sup>Na<sup>+</sup> efflux in voltage-clamped, internally dialyzed giant axons of the squid *Loligo pealei*. The conductance of single palytoxin-bound “pump-channels” in outside-out patches was ~7 pS in symmetrical 500 mM [Na<sup>+</sup>], comparable to findings in other cells. In these high-[Na<sup>+</sup>], K<sup>+</sup>-free solutions, with 5 mM cytoplasmic [ATP], the  $K_{0.5}$  for palytoxin action was ~70 pM. The pump-channels were ~40–50 times less permeable to *N*-methyl-D-glucamine (NMG<sup>+</sup>) than to Na<sup>+</sup>. The reversal potential of palytoxin-elicited current under biionic conditions, with the same concentration of a different permeant cation on each side of the membrane, was independent of the concentration of those ions over the range 55–550 mM. In giant axons, the Ussing flux ratio exponent ( $n'$ ) for Na<sup>+</sup> movements through palytoxin-bound pump-channels, over a 100–400 mM range of external [Na<sup>+</sup>] and 0 to –40 mV range of membrane potentials, averaged  $1.05 \pm 0.02$  ( $n = 28$ ). These findings are consistent with occupancy of palytoxin-bound Na<sup>+</sup>/K<sup>+</sup> pump-channels either by a single Na<sup>+</sup> ion or by two Na<sup>+</sup> ions as might be anticipated from other work; idiosyncratic constraints are needed if the two Na<sup>+</sup> ions occupy a single-file pore, but not if they occupy side-by-side binding sites, as observed in related structures, and if only one of the sites is readily accessible from both sides of the membrane.

## INTRODUCTION

Palytoxin is a potent marine toxin that impairs ATPase activity of the Na<sup>+</sup>/K<sup>+</sup> pump and simultaneously increases cation permeability of mammalian cells (for reviews see Habermann, 1989; Tosteson, 2000). Two lines of evidence initially established that palytoxin interacts with the Na<sup>+</sup>/K<sup>+</sup> pump itself. First, palytoxin elicited ouabain-sensitive cation flux in yeast cells (which lack endogenous Na<sup>+</sup>/K<sup>+</sup> pumps) only after expression of both Na<sup>+</sup>/K<sup>+</sup>-ATPase  $\alpha$  and  $\beta$  subunits, and not of either subunit alone (Scheiner-Bobis et al., 1994). Second, incorporation of in vitro–translated Na<sup>+</sup>/K<sup>+</sup>-ATPase  $\alpha$  and  $\beta$  subunits into lipid bilayers permitted palytoxin to open cation channels with a unitary conductance of ~10 pS (Hirsh and Wu, 1997), similar to that of the relatively nonselective channels opened by palytoxin in the surface membrane of mammalian cells (Ikeda et al., 1988;

Muramatsu et al., 1988). Furthermore, scanning cysteine accessibility measurements (for review see Horisberger, 2004; see also Reyes and Gadsby, 2006) have demonstrated that several positions along the fourth, fifth, and sixth transmembrane helices of the Na<sup>+</sup>/K<sup>+</sup> pump are water accessible in palytoxin-bound “pump-channels.” Amino acids at some of those positions are homologous to ion-coordinating residues in crystal structures of the related Ca<sup>2+</sup>-ATPase (Toyoshima et al., 2000; Møller et al., 2005), and had been assigned cation-binding roles in the Na<sup>+</sup>/K<sup>+</sup> pump on the basis of mutagenesis results (Nielsen et al., 1998; Pedersen et al., 1998). It appears, therefore, that not only is the Na<sup>+</sup>/K<sup>+</sup> pump the target of palytoxin, but the ion pore of the palytoxin-bound pump-channel comprises at least part of the pathway normally negotiated by the pumped Na<sup>+</sup> and K<sup>+</sup> ions.

Additional evidence suggests that current flow through the ion channels opened by palytoxin is controlled by two gates in series that normally alternately regulate access to the ion-binding sites deep within the Na<sup>+</sup>/K<sup>+</sup> pump (Artigas and Gadsby, 2003a; Harmel and Apell, 2006). Thus, the open probability of palytoxin-bound pump-channels can be modified by replacing extracellular Na<sup>+</sup> ions with K<sup>+</sup> ions, or by altering the intracellular [ATP]. Because these are the physiological ligands of the

Correspondence to R.F. Rakowski: rakowski@ohio.edu; or D.C. Gadsby: gadsby@rockefeller.edu

R.F. Rakowski's address is Department of Biological Sciences, Ohio University, Irvine Hall, Athens, OH 45701.

P. Artigas' and D.C. Gadsby's address is Laboratory of Cardiac/Membrane Physiology, Rockefeller University, 1230 York Avenue, New York, NY 10021.

F. Palma's and M. Holmgren's address is National Institutes of Health, NINDS, Bethesda, MD 20892.

P. De Weer's address is Department of Physiology, University of Pennsylvania, School of Medicine, 3700 Hamilton Walk, Philadelphia, PA 19104.

The online version of this article contains supplemental material.

Abbreviations used in this paper: NMG<sup>+</sup>, *N*-methyl-D-glucamine; PPTEA, phenylpropyltriethylammonium.

Na<sup>+</sup>/K<sup>+</sup> pump that drive the conformational changes that underlie its Na<sup>+</sup>/K<sup>+</sup> transport cycle, their influence on the gating of palytoxin-bound pump-channels supports the use of palytoxin as a tool for probing the Na<sup>+</sup>/K<sup>+</sup> pump's ion translocation pathway.

Here we present the results of experiments to further characterize that pathway in Na<sup>+</sup>/K<sup>+</sup> pumps of squid giant axons. Extracellular, but not intracellular, application of palytoxin was shown long ago to depolarize squid axons by rendering them leaky to Na<sup>+</sup> and other small monovalent cations (Pichon, 1982; Muramatsu et al., 1984). We first verified that palytoxin-bound pump-channels in outside-out patches excised from the neurons that give rise to the squid giant axons displayed characteristics comparable to those observed in mammalian cells. We then exploited those characteristics to examine both unidirectional and net Na<sup>+</sup> ion movement through palytoxin-bound pump-channels in voltage-clamped, internally dialyzed squid giant axons. Although it is well known that, in its E1P conformation, the Na<sup>+</sup>/K<sup>+</sup> pump is capable of binding up to three Na<sup>+</sup> ions and of occluding them inside the protein core (for review see Glynn and Karlish, 1990), evidence suggests that palytoxin stabilizes an E2P-like conformation (Artigas and Gadsby, 2004; Harmel and Apell, 2006; Reyes and Gadsby, 2006) that, during the normal transport cycle, occludes two K<sup>+</sup> or Na<sup>+</sup> ions (Glynn and Karlish, 1990; Sturmer and Apell, 1992). Interestingly, we found that the Ussing flux ratio exponent,  $n'$ , was close to 1.0 for palytoxin-bound pump-channels in all experimental conditions tested. We speculate how the characteristic side-by-side arrangement of the ion-binding sites in this family of P-type ATPases might result in an ion pathway that, when both gates are open, behaves like an ion channel rarely occupied by more than one ion.

## MATERIALS AND METHODS

### Isolation and Culture of Giant Fiber Lobe Neurons

Neuronal cell bodies of the squid, *Loligo pealei*, were dissociated following Llano and Bookman (1986) and Gilly et al. (1990). In brief, the giant fiber lobe dissected from the stellate ganglion was incubated for 40–45 min in filtered sea water containing 10 mg/ml of protease Type XIV (Sigma-Aldrich). After several washes with fresh sea water, the lobe was placed in culture medium and the cells were dispersed by gentle mechanical disruption with a fire-polished glass pipette. Dispersed cells were seeded onto glass coverslips that had been immersed in ethanol, flamed, and treated with poly-L-lysine overnight (1 mg/ml in 0.15 M Trizma, pH 8.5). The cell culture medium was Leibovitz L-15 (GIBCO BRL) supplemented with (in mM) 263 NaCl, 4.6 KCl, 9 CaCl<sub>2</sub>, 50 MgCl<sub>2</sub>, 2 HEPES, 2 L-glutamine, 6% FBS (GIBCO BRL), 50 U/ml penicillin, and 50 mg/ml streptomycin; pH 7.8 with NaOH. Cells were incubated at 17°C and used for recording within the first week of culture.

### Patch Recording Methods and Solutions

Currents in outside-out patches (Hamill et al., 1981) were recorded at room temperature (19–23°C) using pipettes pulled from borosilicate glass (PG52151–4; WP Instruments) with a horizontal puller (P90; Sutter Instruments) and with tips coated with

Sylgard. When filled with 500 mM Na<sup>+</sup> solution, the pipette had a resistance of 1.5–12 MΩ for macroscopic, or 7–40 MΩ for single-channel current recordings. Currents were recorded with an Axopatch 200B amplifier, filtered at 1 kHz (8 pole Bessel), and sampled at 5 kHz using a Digidata 1322A A/D converter and pClamp 9 software, and also continuously acquired in parallel at lower rates with a Minidigi 1A and Axoscope 9 (Axon Instruments, Inc.). Single-channel current records were digitally filtered at 100 Hz and baseline drifts were subtracted using Clampfit 9.

External solutions used for measuring single-channel conductance and evaluating concentration dependence of palytoxin action in patches contained (in mM) ~520 or ~560 sulfamic acid, 460 or 500 NaOH (as specified in figure legends), 10 CaCl<sub>2</sub>, 40 Mg(OH)<sub>2</sub>, and 10 HEPES; NaOH was replaced with equimolar KOH or *N*-methyl-D-glucamine (NMG<sup>+</sup>) in Na<sup>+</sup>-free solutions. The internal (pipette) solution contained (in mM) 470 sulfamic acid, 500 NaOH, 10 phenylpropyltriethylammonium (PPTEA)-SO<sub>4</sub>, 10 MgCl<sub>2</sub>, 5 Tris-ATP, 10 EGTA, and 20 HEPES (for most single-channel recordings, 9 MgCl<sub>2</sub> was replaced with 9 Mg-sulfamate to improve signal-to-noise ratio). For determination of biionic reversal potentials, external solutions contained (in mM) 540 sulfamic acid, 550 NaOH or tetramethylammonium (TMA)OH, 1 CaCl<sub>2</sub>, 2 MgCl<sub>2</sub>, and 10 HEPES, and the internal solution contained (in mM) 520 sulfamic acid, 550 NaOH, 10 PPTEA bromide, 2 MgCl<sub>2</sub>, 1 Tris-ATP, 10 EGTA, and 10 HEPES. Other external and internal Na<sup>+</sup> (or TMA<sup>+</sup>) concentrations were obtained by isoosmotic replacement of Na<sup>+</sup> (or TMA<sup>+</sup>) sulfamate with sucrose. The osmolality of all solutions in patch recording experiments was 970–1,000 mOsm kg<sup>-1</sup>, their pH was 7.4, and all external solutions contained 0.2 μM TTX.

### Solutions for Internal Dialysis

The standard external solution contained (in mM) 400 Na isethionate, 75 Ca sulfamate, 0.1 Tris EDTA, 5 Tris HEPES (pH 7.7), 1 3,4-diaminopyridine, and 0.2 μM TTX. In Na<sup>+</sup>-free external solutions, Na isethionate was replaced with 400 mM NMG sulfamate or 400 K sulfamate; the Na<sup>+</sup> and NMG<sup>+</sup> solutions were mixed to vary [Na<sup>+</sup>], and external solutions containing both Na<sup>+</sup> and K<sup>+</sup> were obtained by mixing or by adding K<sup>+</sup> from a 0.5M K-sulfamate stock solution. The internal dialysate contained (in mM) 100 Na HEPES, 20 NMG HEPES, 50 glycine, 50 PPTEA-SO<sub>4</sub>, 5 dithiothreitol, 50 BAPTA NMG, 10 Mg HEPES, 5 MgATP, 5 NMG phosphoenolpyruvate, and 5 NMG phosphoarginine, pH ~7.5, and <sup>22</sup>Na<sup>+</sup> as needed. The osmolalities of dialysate and extracellular solutions were adjusted to be the same, within 1%, and were ~930 mOsm kg<sup>-1</sup>.

### Measurement of Net Membrane Current and Unidirectional <sup>22</sup>Na<sup>+</sup> Flux

Simultaneous measurements of membrane current and <sup>22</sup>Na<sup>+</sup> efflux in voltage-clamped, internally dialyzed *Loligo pealei* giant axons were as previously described (Rakowski, 1989; Rakowski et al., 1989). A 23-mm segment of squid giant axon, cannulated at both ends, was threaded with a cellulose acetate capillary rendered porous to low molecular weight solutes to allow internal dialysis, a blackened Pt wire for passing current, and a 3 M KCl-filled glass capillary electrode for recording voltage. The voltage difference between this internal electrode positioned in the middle of the axon segment and an external flowing 3 M KCl reference electrode positioned near the solution outflow was controlled by a stable, low noise voltage clamp (Rakowski, 1989). The experimental chamber consisted of two lateral pools containing the cannulated axon ends and a central pool, physically separated by grease seals. The central pool was superfused with the external experimental solution kept at 21–22°C. The end and central pools were kept at the same potential by two ancillary voltage clamp circuits to prevent current flow between them. The superfusate from the central pool was collected and the efflux of <sup>22</sup>Na<sup>+</sup> across the

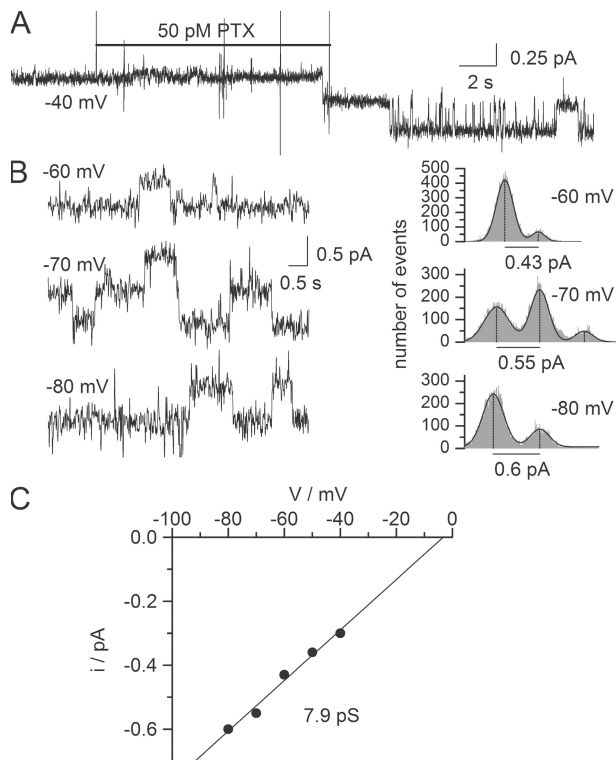


**Figure 1.** Conductance of the palytoxin-bound Na/K pump-channels in squid. (A) Outside-out patch from a giant fiber lobe neuron held at  $-40$  mV with symmetrical  $500$  mM  $\text{Na}^+$ . The patch showed no endogenous channel activity before the exposure to  $50$  pM palytoxin. After  $\sim 12$  s of exposure to palytoxin, the first Na/K pump-channel opened, immediately following which the toxin was removed. During toxin washout, a second pump-channel opened. (B) Current records acquired at holding potentials of  $-60$ ,  $-70$ , and  $-80$  mV are shown on the left and the corresponding current amplitude histograms on the right. Histograms were fitted with multiple-peak Gaussian functions (solid lines) to estimate the single-channel current amplitude at each potential. (C) Voltage dependence of the single-channel current. Solid line represents a least-squares straight line fit with a slope of  $7.9 \pm 0.6$  pS.

axon membrane in the experimental region was measured by either liquid scintillation or gamma counting. Where shown, data points and error bars indicate the mean  $\pm$  SEM.

#### Online Supplemental Material

The supplemental material is available at <http://www.jgp.org/cgi/content/full/jgp.200709770/DC1>. Fig. S1 demonstrates that TTX-sensitive current and  $^{22}\text{Na}^+$  efflux are equivalent in a squid axon under zero-trans conditions, confirming that they emanate from the same controlled area of axon membrane. Fig. S2 illustrates simultaneous measurements of current and  $^{22}\text{Na}^+$  efflux flowing through palytoxin-opened Na/K pump-channels during four consecutive applications of palytoxin to a single axon, at three different membrane potentials.

## RESULTS

### Conductance of Single Palytoxin-bound Pump-Channels

We first examined characteristics of palytoxin-bound squid  $\text{Na}^+/\text{K}^+$  pump-channels in membrane patches

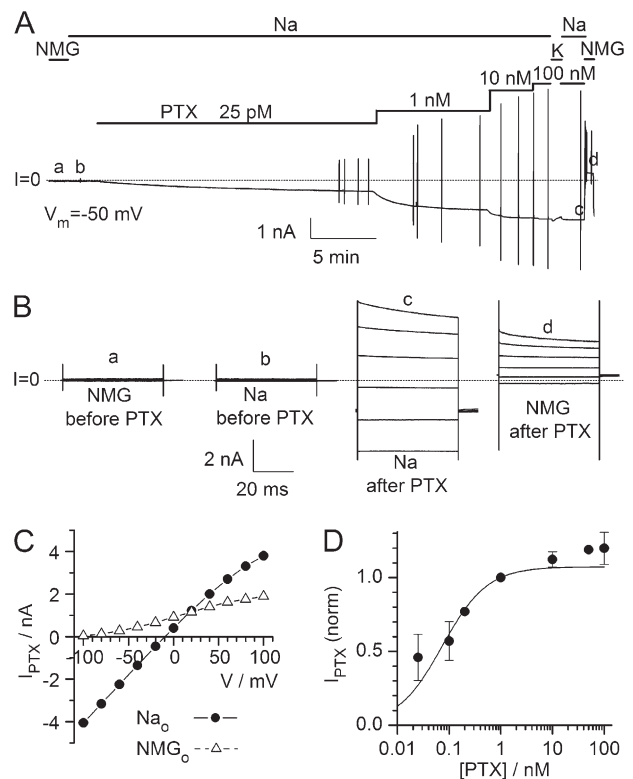


**Figure 2.** Apparent affinity for palytoxin. (A) Outside-out patch from a giant fiber lobe neuron held at  $-50$  mV. Top, horizontal bars designate bath ionic composition and the concentration of palytoxin used. Bottom, current trace. The dotted line indicates the zero current level. Palytoxin concentrations were increased when approximately steady current levels were reached at each dose. The brief vertical deflections in the current record indicate  $I$ - $V$  measurements. (B) Membrane current traces in response to  $50$  ms voltage steps from  $-100$  to  $100$  mV (displayed here in  $40$ -mV increments) in external solutions containing  $\text{NMG}^+$  or  $\text{Na}^+$  before (a and b) and after complete treatment with palytoxin (c and d). (C) Average palytoxin-induced current ( $I$  after palytoxin minus  $I$  before palytoxin) during the last  $5$  ms of every pulse under each ionic condition plotted against the applied voltage. The relative permeability of  $\text{NMG}^+$  ( $P_{\text{NMG}^+}/P_{\text{Na}^+}$ ) was  $0.024 \pm 0.002$  as calculated from the large shift in reversal potential ( $\Delta V_{\text{rev}} = -94 \pm 2$  mV). (D) Normalized and averaged dose response curve for palytoxin obtained from six patches. The solid line represents a Michaelis-Menten equation fit with a  $K_{0.5} = 74 \pm 21$  pM.

excised from enzymatically dissociated giant-fiber lobe neurons, the neurons in the stellate ganglion whose axons fuse to form the giant axons. In outside-out patches, with  $500$  mM  $\text{Na}^+$  on both sides of the membrane and  $5$  mM ATP in the pipette, exposure to picomolar concentrations of palytoxin allowed individual  $\text{Na}^+/\text{K}^+$  pump-channel transformation events to be detected as tiny inward current steps at negative membrane potentials (Fig. 1 A). Because palytoxin remains tightly bound, the pump-channels continued to open and close long after patches were washed free of unbound toxin (Fig. 1, A and B). This allowed measurements of current steps at several voltages (Fig. 1 B) and construction of single-channel

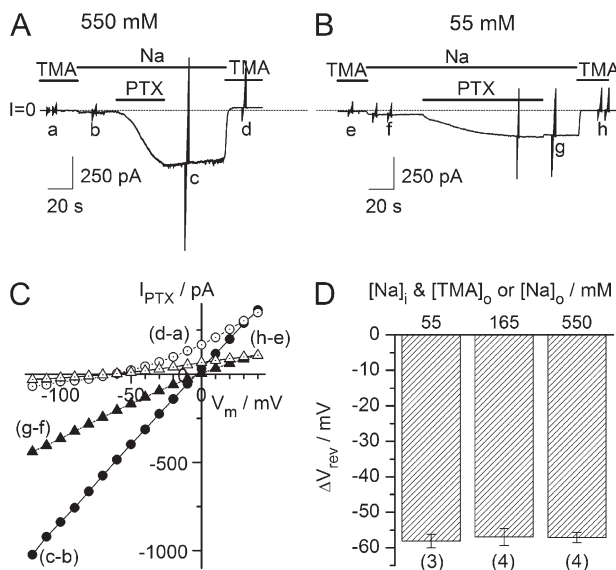


**Figure 3.** The  $\text{Na}^+/\text{TMA}^+$  biionic potential is independent of the absolute concentration of these permeant ions. (A and B) Outside-out patches from giant fiber lobe neurons held at  $-50$  mV with pipettes containing 550 (A) or 55 (B) mM  $\text{Na}^+$ . Top, horizontal bars designate bath ionic composition and application of palytoxin (10 nM). Bottom, current trace; the dotted line indicates the zero current level, and the brief vertical deflections indicate episodes in which 50-ms-long voltage pulses ( $-120$  to  $+40$  mV in 10-mV increments) were applied. (C) Palytoxin-induced  $I$ - $V$  relationships with bath solutions containing 550 mM  $\text{Na}^+$  (from A; filled circles, c-b), 550 mM  $\text{TMA}^+$  (from A; open circles, d-a), 55 mM  $\text{Na}^+$  (from B; filled triangles, g-f) and 55 mM  $\text{TMA}^+$  (from B; open triangles, h-e). (D) Changes in  $V_{rev}$  ( $V_{rev}\text{TMA}^+_{\text{o}} - V_{rev}\text{Na}^+_{\text{o}}$ ) at three different permeant ion concentrations. Mean values (number of experiments given in parentheses) were  $-58 \pm 2$ ,  $-57 \pm 3$ , and  $-57 \pm 1$  mV for permeant ion concentrations of 55, 165, and 550 mM, respectively.

current-voltage curves (e.g., Fig. 1 C). Single pump-channel conductance measured in this way in five patches averaged  $7.4 \pm 0.2$  pS.

#### Palytoxin Apparent Affinity

With symmetrical  $[\text{Na}^+]_i$  and ATP in the pipette, exposure of outside-out patches to stepwise increasing concentrations of palytoxin caused a progressive inward current increase at  $-50$  mV, reflecting eventual transformation of every  $\text{Na}^+/\text{K}^+$  pump in the patch into a cation channel (Fig. 2 A). Complete replacement of external  $\text{Na}^+$  with  $\text{NMG}^+$  after that transformation caused a large outward current shift (Fig. 2, A and B), due to the slower permeation of the larger  $\text{NMG}^+$  cation through palytoxin-bound pump-channels. Current flowing through the palytoxin-bound pump-channels was estimated by appropriate subtraction of currents averaged over the final 5 ms of 50-ms steps to voltages between  $-100$  and  $+100$  mV (in 20-mV increments), in external  $\text{Na}^+$  and in external  $\text{NMG}^+$ , before (Fig. 2 B, a and b) and after (Fig. 2 B, c and d) exposure to palytoxin. The resulting palytoxin-induced current is shown

plotted against voltage in Fig. 2 C. From the large negative shift of reversal potential ( $\Delta V_{rev} = -94 \pm 2$  mV,  $n = 3$ ) upon replacing external  $\text{Na}^+$  with  $\text{NMG}^+$ , the relative permeability  $P_{\text{NMG}}/P_{\text{Na}}$  was calculated to be  $0.024 \pm 0.002$ . The smaller outward current at large positive potentials suggests that extracellular  $\text{NMG}^+$  impaired the outward flow of  $\text{Na}^+$  ions through palytoxin-bound pump-channels.

Amplitudes of steady palytoxin-induced currents at several palytoxin concentrations, normalized to the current elicited by 1 nM palytoxin in the same patch, are summarized in Fig. 2 D in which the Michaelis-Menten fit yields a  $K_{0.5}$  of  $74 \pm 21$  pM ( $n = 6$ ). Current decayed slowly after palytoxin removal (not depicted) and, in  $\text{Na}^+$  solution, followed a single exponential time course ( $\tau = 770 \pm 260$  s,  $n = 3$ ). But current decay upon replacing external  $\text{Na}^+$  with  $\text{K}^+$  was faster and required two exponentials with time constants  $\tau_f = 40 \pm 10$  s and  $\tau_s = 400 \pm 120$  s (with fractional amplitudes  $A_f = 0.55 \pm 0.05$  and  $A_s = 0.45 \pm 0.05$ ,  $n = 3$ ).

#### Biionic Reversal Potentials ( $\text{TMA}^+_{\text{o}}/\text{Na}^+_{\text{i}}$ ) Are Independent of the Absolute Concentration of the Two Permeant Ions

One test for multiple ion occupancy of single-file pores is to examine their reversal potentials under biionic conditions, but with different values for the identical concentrations of the two permeant ions on opposite sides of the membrane. If a single-file channel is occupied by at most one ion, the biionic reversal potential is expected to remain constant, independent of the absolute ion concentrations (Läuger, 1973; Levitt, 1986; Zarei and Dani, 1994).

Because  $\text{TMA}^+$  is somewhat more permeant than  $\text{NMG}^+$  in palytoxin-bound pump-channels (Artigas and Gadsby, 2004), we paired internal  $\text{Na}^+$  with external  $\text{TMA}^+$  (instead of  $\text{NMG}^+$ ) to more accurately measure reversal potentials. The reversal potential in nominally symmetrical  $\text{Na}^+$  solutions ( $[\text{Na}^+] = 55, 165, \text{ or } 550$  mM) averaged  $0.1 \pm 0.7$  mV ( $n = 11$ ). We determined biionic potentials in each patch as the reversal potential shift ( $\Delta V_{rev}$ ) on quickly switching from the  $\text{Na}^+$ -containing external solution to one containing the same concentration of  $\text{TMA}^+$ . Fig. 3 (A and B) shows examples of palytoxin-induced currents activated in outside-out patches initially exposed to symmetrical solutions containing 550 mM  $\text{Na}^+$  (A) or 55 mM  $\text{Na}^+$  (B). The corresponding, roughly linear, palytoxin-induced current-voltage curves, with reversal potentials close to 0 mV (Fig. 3 C, filled symbols), were obtained by subtraction of currents recorded during voltage-step episodes marked b and c, and f and g, respectively. Equivalent palytoxin-induced current-voltage curves at the same internal  $\text{Na}^+$  concentrations, but after switching to external solutions containing 550 mM (Fig. 3 A) or 55 mM (Fig. 3 B)  $\text{TMA}^+$ , were obtained by subtracting currents from episodes a and d, and e and h, respectively,

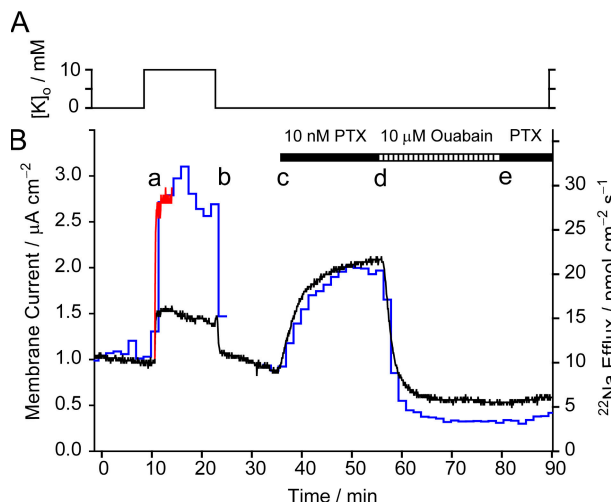


**Figure 4.** Palytoxin-induced current and  $^{22}\text{Na}^+$  efflux under zero-trans conditions. The axon was internally dialyzed with 93 mM  $\text{Na}^+$ , superfused with 400 mM NMG $^+$ ,  $\text{Na}^+$ - and  $\text{K}^+$ -free solution, and voltage clamped at  $-20$  mV. Membrane current (noisy solid trace) and  $^{22}\text{Na}^+$  efflux (blue lines, 1.5-min sample intervals) were measured simultaneously. To allow direct comparison of changes in current and flux they are plotted at equivalent vertical gain and the baseline current was set equal to the flux at time zero. At a, 10 mM  $\text{K}^+$  was added to the  $\text{Na}^+$ -free solution to activate the  $\text{Na}^+$ ,  $\text{K}^+$ -ATPase. The red line shows that three times the change in current on adding 10 mM  $\text{K}^+$  is equivalent to the change in  $^{22}\text{Na}^+$  efflux, as expected for a pump stoichiometry of 3  $\text{Na}^+$ /2  $\text{K}^+$ . The solution was changed back to  $\text{Na}^+$ - and  $\text{K}^+$ -free at b. At c, 10 nM palytoxin was added to the superfusate. At d, palytoxin was omitted and 10  $\mu\text{M}$  ouabain was added. At e, ouabain was omitted and 10 nM palytoxin restored.

which yielded reversal potentials negative to  $-50$  mV. On average,  $\Delta V_{rev}$  upon replacing external  $\text{Na}^+$  with TMA $^+$  (Fig. 3 D) was the same at ion concentrations of 55 mM ( $-58 \pm 2$  mV), 165 mM ( $-57 \pm 3$  mV), and 550 mM ( $-57 \pm 1$  mV), indicating that  $P_{TMA}/P_{Na}$  was concentration independent over this range, with a mean value of  $0.102 \pm 0.004$  ( $n = 11$ ).

#### Correspondence of Simultaneously Measured Electrical Current and Radiotracer Flux

To accurately compute unidirectional  $\text{Na}^+$  influx from measurements of net electrical current and unidirectional  $^{22}\text{Na}^+$  efflux, measured current and tracer flux must derive from the same area of membrane. In voltage-clamped internally dialyzed giant axons treated with veratridine and bathed in  $\text{Na}^+$ -free external solution, we have previously demonstrated equivalence of the TTX-inhibited steady net outward current and the TTX-sensitive unidirectional  $^{22}\text{Na}^+$  efflux, in experiments lasting  $\sim 15$  min (Rakowski et al., 1989). This is the expected result for electrodiffusive  $\text{Na}^+$  ion flow through  $\text{Na}^+$ -selective channels under zero-trans conditions, and so it confirmed that current and flux were measured from the same population of channels. An

experiment showing that the same holds true for measurements of longer duration ( $\sim 40$  min), similar to those needed in the palytoxin experiments described below, is illustrated in Fig. S1 (available at <http://www.jgp.org/cgi/content/full/jgp.200709770/DC1>).

#### Under Zero-Trans Conditions ( $\text{Na}^+$ -free External Solution) Palytoxin-induced $^{22}\text{Na}^+$ Efflux and Outward Current Have the Same Size and Time Course

As established for  $\text{Na}^+$  ion movement via TTX-sensitive channels, Fig. 4 confirms that under zero-trans conditions, unidirectional  $\text{Na}^+$  efflux and net current flowing through palytoxin-bound pump-channels are also equivalent. When this axon, held at  $-20$  mV, with  $\sim 100$  mM internal  $\text{Na}^+$  and in  $\text{Na}^+$ -free, NMG $^+$ -containing external solution, was exposed (at c) to 10 nM palytoxin, outward current (continuous noisy black trace) and  $^{22}\text{Na}^+$  efflux (determined at 1.5-min intervals; blue line) increased promptly and in parallel; their time courses and amplitudes (after scaling by Faraday's constant) were the same, as expected if they derive from the same population of palytoxin-bound  $\text{Na}^+$ / $\text{K}^+$  pump-channels.

Like ouabain's action to shut palytoxin-bound  $\text{Na}^+$ / $\text{K}^+$  pump-channels in mammalian cells and accelerate dissociation of palytoxin (Artigas and Gadsby, 2004), in squid axon, too, withdrawal of palytoxin and addition of 10  $\mu\text{M}$  ouabain (at d in Fig. 4) resulted in rapid, near parallel decreases of both outward current and  $^{22}\text{Na}^+$  efflux. The ouabain-induced decrement of  $^{22}\text{Na}^+$  efflux was slightly larger than that of the current, and both reached smaller values than observed before palytoxin. These differences possibly reflect abolition by ouabain of not only the palytoxin-induced signals but also a low level of electrogenic  $\text{Na}^+$ / $\text{K}^+$  pump activity (with  $\text{Na}^+$  efflux/current ratio of 3/1) supported by contaminating  $\text{K}^+$  in the nominally  $\text{K}^+$ -free and  $\text{Na}^+$ -free, but 400 mM NMG $^+$ -containing, external solution (Rakowski et al., 1989). That this axon was indeed capable of producing changes in  $^{22}\text{Na}^+$  efflux and current of the expected relative magnitudes upon  $\text{Na}^+$ / $\text{K}^+$  pump activation, by addition of 10 mM external  $\text{K}^+$ , is shown by comparison of the increments of  $^{22}\text{Na}^+$  efflux and current initiated at a. The ratio of the pump-mediated changes in flux and current ( $F\Delta\Phi_{out}/\Delta I$ ) calculated from these increments (measured as in Rakowski et al., 1989) was 2.94, near the value of 3.0 expected for 3  $\text{Na}^+$ :2  $\text{K}^+$  exchange. The red trace shows the recorded change in current multiplied by 3.0, to allow direct visual comparison with the simultaneous change in  $^{22}\text{Na}^+$  efflux. This close agreement with expectation further corroborates that measured flux and current originate from the same area of axon membrane.

A subsequent  $\sim 20$ -min re-exposure to 10 nM palytoxin (beginning at e), with concomitant withdrawal of ouabain, failed to transform any pumps into ion channels, presumably because they were protected by persistently

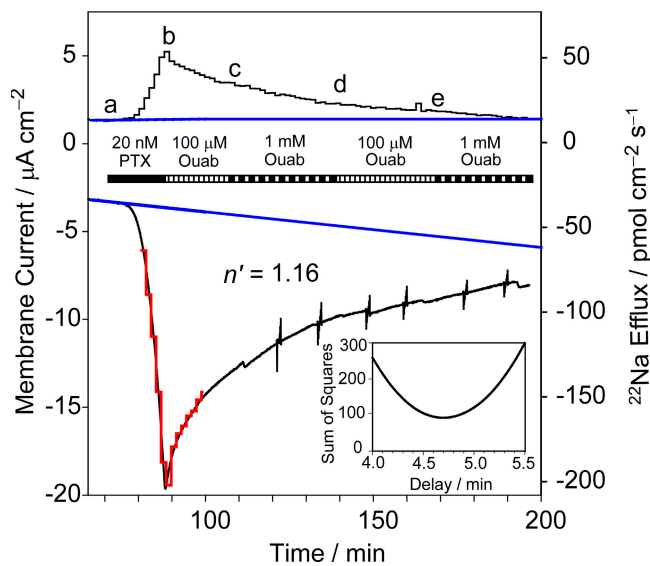


**Figure 5.** Determination of the flux ratio exponent  $n'$  for Na/K pump-channels opened by palytoxin. The axon was internally dialyzed with 98 mM  $\text{Na}^+$  and superfused with 400 mM  $\text{Na}^+$ , and held at 0 mV. Simultaneous measurements of unidirectional  $^{22}\text{Na}^+$  efflux (top trace) and net current (bottom trace) were used to estimate the flux ratio exponent  $n'$  for Na/K pump-channels opened by 20 nM palytoxin. The inset figure illustrates the procedure to account for the delay between current measurements and the fraction collector that collected radioactive samples. Least-squares fits of Eq. 1 to the current and flux data were repeated for successive 5-s increments of delay, to find the delay time that minimized the sum of squared deviations for the estimate of  $n'$ . In this experiment, a time delay of 4.70 min resulted in a minimum in the sum of squares and gave an estimate for  $n'$  of 1.16. Baseline values (blue lines) for  $^{22}\text{Na}^+$  efflux and net current were used to correct measured values in the determinations of  $n'$ . The red trace represents the measured efflux data transformed by Eqs. 1 and 2 using the best-fit  $n'$  and delay value obtained from the fits. In the presence of external  $\text{Na}^+$ , saturating concentrations of ouabain fully reverse palytoxin-induced  $^{22}\text{Na}^+$  efflux in  $\sim 100$  min. Vertical current displacements are in response to voltage staircases, with 0.5 mV steps, from  $-5$  to 5 mV applied to monitor membrane conductance during the decline in current and flux.

bound ouabain under these conditions (but see Figs. 7 and 8, below).

#### Action of Palytoxin and Ouabain in 400 mM $[\text{Na}^+]$ , $\text{K}^+$ -free, External Solution

At high (400 mM) external  $\text{Na}^+$ , responses to 20 nM palytoxin applied to an axon, held at 0 mV, and with  $\sim 100$  mM internal  $\text{Na}^+$ , appeared larger (Fig. 5) than expected from the results in  $\text{Na}^+$ -free  $\text{NMG}^+$  external solution (e.g., Fig. 4). In the axon of Fig. 5, before its accelerating action was precipitously interrupted by addition of 100  $\mu\text{M}$  ouabain, palytoxin activated  $>35$  (compared with  $\sim 15$ )  $\text{pmol cm}^{-2} \text{ s}^{-1}$  of  $^{22}\text{Na}$  efflux within 10 min, and a net current ( $\geq 15 \mu\text{A cm}^{-2}$ ) that was larger than predicted, assuming independence. The smaller response in Fig. 4 likely reflects partial block of palytoxin-bound pump-channels by external  $\text{NMG}^+$ , as observed in outside-

out patches (Fig. 2 C). A further contrast with Fig. 4 is the order-of-magnitude slower reversal of palytoxin action upon its withdrawal in the presence of saturating concentrations of ouabain (1 mM was no more effective than 100  $\mu\text{M}$ ; Fig. 5). The palytoxin pump complex is evidently stabilized at high external  $[\text{Na}^+]$  (compare Artigas and Gadsby, 2004).

#### Calculation of the Ussing Flux Ratio Exponent, $n'$

Measurement of the unidirectional ion flows through an ion-selective pore, in both directions, and estimation of the Ussing flux ratio exponent,  $n'$ , provides information about the average number of ions inside the pore at any instant (Ussing, 1949; Hodgkin and Keynes, 1955; Kohler and Heckmann, 1979). We previously measured  $n'$  for TTX-sensitive  $\text{Na}^+$  channels in squid axons and obtained a value of  $0.97 \pm 0.03$  (Rakowski et al., 2002). For such  $\text{Na}^+$ -selective channels, simultaneous measurement of unidirectional  $^{22}\text{Na}^+$  efflux ( $\Phi_{out}$ ) and net current ( $I$ ) allows calculation of unidirectional  $\text{Na}^+$  influx ( $\Phi_{in}$ ) by difference and, hence, determination of the ratio of unidirectional fluxes. The flux ratio exponent  $n'$  can then be computed from

$$\frac{\Phi_{out}}{\Phi_{in}} = \left( \frac{[\text{Na}^+]_i}{[\text{Na}^+]_o} \cdot e^{\frac{VF}{RT}} \right)^{n'} \quad (1)$$

where  $[\text{Na}^+]_i$  and  $[\text{Na}^+]_o$  are the internal and external  $\text{Na}^+$  concentrations,  $V$  is the membrane potential, and  $R$ ,  $T$  and  $F$  have their usual meanings.

Although palytoxin-bound pump-channels select poorly among small monovalent cations (Ikeda et al., 1988; Muramatsu et al., 1988; Tosteson et al., 1991; Artigas and Gadsby, 2004), under the conditions of these experiments,  $\text{Na}^+$  ions are the principal charge carriers. This is because  $\text{Na}^+$  ions are  $\sim 50$ -fold more permeant than  $\text{NMG}^+$  (Fig. 2; Artigas and Gadsby, 2004) or  $\text{Ca}^{2+}$  (Rouzaire-Dubois and Dubois, 1990; Artigas and Gadsby, 2004), the other major cations present. The observed correspondence between palytoxin-induced outward current and unidirectional  $\text{Na}^+$  efflux into  $\text{Na}^+$ -free external solution (Fig. 4) supports the essentially  $\text{Na}^+$ -selective behavior of palytoxin-bound pump-channels in these conditions. So, on the assumption that  $\text{Na}^+$  was the charge-carrying species, we used the measured palytoxin-elicited increments in unidirectional efflux ( $\Delta\Phi_{out}$ ) and net current ( $\Delta I$ ) to calculate the palytoxin-induced increment in unidirectional  $\text{Na}^+$  influx ( $\Delta\Phi_{in}$ ),

$$\Delta\Phi_{in} = (\Delta I / F) - \Delta\Phi_{out} \quad (2)$$

and then substituted the ratio  $\Delta\Phi_{out}/\Delta\Phi_{in}$  for  $\Phi_{out}/\Phi_{in}$  in Eq. 1 to compute the flux ratio exponent  $n'$  for the channels opened by palytoxin.

In the experiment of Fig. 5, with 400 mM  $\text{Na}^+_o$  and  $\sim 100$  mM  $\text{Na}^+_i$  and the axon held at 0 mV, an efflux/

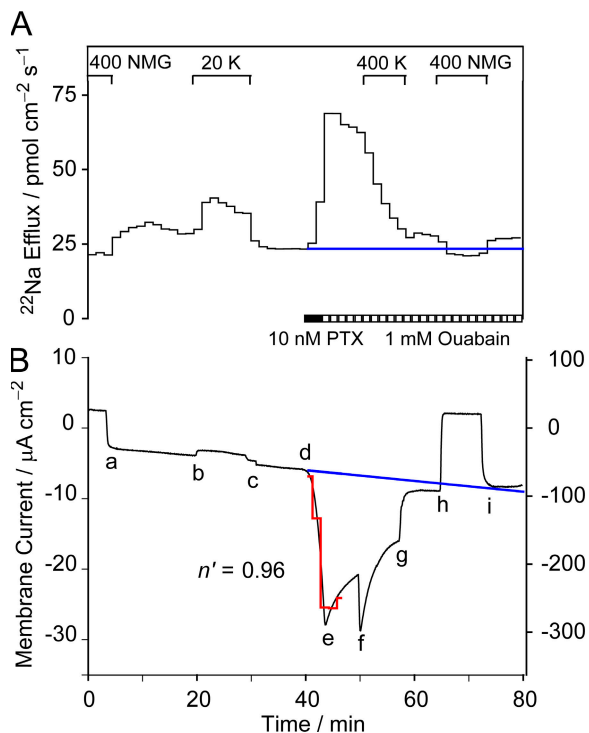


**Figure 6.** External  $K^+$  speeds the closure of Na/K pump-channels opened by palytoxin. The axon was internally dialyzed with 94 mM  $Na^+$  and held at 0 mV throughout the measurements of (A)  $^{22}Na^+$  efflux and (B) net membrane current. A detailed description of the experiment is given in the text. Blue lines indicate the extrapolated baselines for  $^{22}Na^+$  efflux and net current. The red trace represents the measured efflux data transformed by Eqs. 1 and 2 using the best-fit  $n'$  value of 0.96 and least-squares delay obtained as described in Fig. 5. After a saturating concentration of ouabain partially reverses palytoxin action, replacement of all external  $Na^+$  with  $K^+$  fully restores baseline current and  $^{22}Na^+$  efflux levels in  $\sim 10$  min.

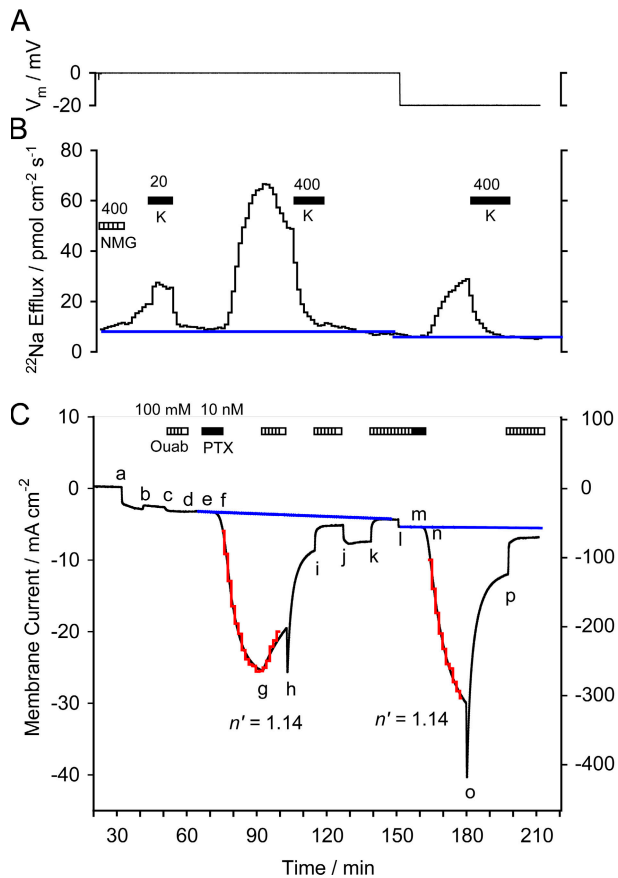
influx ratio of 0.25 ( $100/400$ ) is expected if the Ussing flux ratio exponent were 1.0. An initial estimate of  $n'$  can be garnered as follows. The peak increase in inward current caused by palytoxin was  $16.0 \mu A cm^{-2}$  (equivalent to  $165.8 pmol cm^{-2} s^{-1}$ ), and the peak increase in  $Na^+$  efflux was  $40.4 pmol cm^{-2} s^{-1}$ , giving a calculated peak change in influx equivalent to  $206.2 pmol cm^{-2} s^{-1}$ . Thus the peak response gives an efflux/influx ratio of 0.20, expected (via Eq. 1) for  $n' \sim 1.14$ . As  $n'$  must be independent of the fraction of open pump-channels, a similar calculation can be repeated for each pair of palytoxin-induced current and flux measurements, made at 1.5-min intervals, during the activation or deactivation time course. In practice, all data pairs within a given time period were simultaneously least-squares fit to yield a single estimate for  $n'$ . The period (marked by red traces, see below) was chosen to allow reliable extrapolation of baseline (e.g., straight blue lines in Fig. 5) values of current and  $^{22}Na^+$  efflux and to ensure that palytoxin-induced increments in current and flux were of significant magnitude. The procedure illustrated in

Fig. 5 inset was used to synchronize the current and efflux records, to account for the (imprecisely known) delay between experimental chamber and the fraction collector that collected radioactive samples. The least-squares fit was repeated for successive 5-s increments of assumed delay, to find the delay time that minimized the sum of squared deviations for the estimate of  $n'$ ; in the inset of Fig. 5 this occurred for a time delay of 4.70 min and gave  $n' = 1.16$ . This method of synchronization was employed for all estimations of  $n'$  reported here. The time period over which current and flux data were analyzed to calculate  $n'$  in Figs. 5–9 and Fig. S2 is indicated by the red traces, which represent the measured efflux data, transformed using Eqs. 1 and 2 and the best-fit  $n'$  to generate a “computed current,” and plotted over the measured current after synchronization by the least-squares delay. The superposition illustrates the goodness of fit.

#### Effects of $Na^+$ , $K^+$ , and Ouabain on Palytoxin-induced Current and Flux

In Fig. 6, to more clearly display small changes, the flux ordinate (Fig. 6 A) is expanded relative to that for current (Fig. 6 B). In the initial absence of external  $K^+$ , with  $\sim 100$  mM  $Na^+_i$  and the axon held at 0 mV, raising  $Na^+_o$  from 0 to 400 mM (at a) resulted in transactivation of  $^{22}Na^+$  efflux (reflecting, in part, pump-mediated  $Na^+/Na^+$  exchange) and an inward net current shift (attributable to electrogenic  $Na^+$  flow through unidentified, non-TTX-sensitive, pathways). Addition (at b), followed shortly after by removal (at c), of 20 mM  $K^+_o$  then temporarily converted pump-mediated activity to electrogenic  $Na^+/K^+$  exchange (whose maximum rate exceeds that of  $Na^+/Na^+$  exchange via the pump; Gadsby et al., 1993), resulting in a temporary further increment of  $Na^+$  efflux accompanied by a, similarly temporary, small pump-mediated outward current shift.

Next, addition of 10 nM palytoxin in 400 mM  $Na^+_o$  (at d, in Fig. 6) elicited rapid increases in inward current and in  $^{22}Na^+$  efflux, which stopped upon palytoxin withdrawal (at e) and simultaneous addition of 1 mM ouabain. Replacing 400 mM  $Na^+_o$  with 400 mM  $K^+_o$  (at f), still in 1 mM ouabain, then greatly accelerated recovery from palytoxin. That switch to  $K^+$  was marked by an initial, near instantaneous, increase in inward current owing to the greater permeability of palytoxin-bound pump-channels to  $K^+$  than to  $Na^+$  (by  $\sim 20\%$  in mammalian  $Na^+/K^+$  pumps; Artigas and Gadsby, 2003b, 2004).  $K^+_o$ -induced closure of a large fraction of palytoxin-bound pump-channels was then reflected in rapid decreases in  $^{22}Na^+$  efflux and in inward current (Artigas and Gadsby, 2003a). Restoration of 400 mM  $Na^+_o$  (at g), still with 1 mM ouabain, did not reopen the pump-channels that had been closed by  $K^+$ , confirming that palytoxin had dissociated from those closed channels (Artigas and Gadsby, 2003a). Instead, the switch back



**Figure 7.** Membrane potential does not alter the flux ratio exponent  $n'$ . The axon was internally dialyzed with 99 mM  $\text{Na}^+$  and exposed twice to palytoxin, at two different membrane potentials, 0 and  $-20$  mV. (A) Membrane potential. (B)  $^{22}\text{Na}^+$  efflux. (C) Net membrane current. The experiment is described in detail in the text. Use of 400 mM external  $\text{K}^+$  to accelerate recovery from its action permitted more than one exposure to palytoxin. Blue and red lines have the same meaning as in previous figures.

from  $\text{K}^+$  to  $\text{Na}^+$  caused a slowing of the decline of  $^{22}\text{Na}^+$  efflux, and a decrease in inward current largely due to the smaller permeability to  $\text{Na}^+$  than to  $\text{K}^+$  of residual open pump-channels. The eventual near-complete recovery from the action of palytoxin is shown by the return of the current (after i) to the extrapolated baseline level. The switches between  $\text{Na}^+$ - and  $\text{NMG}^+$ -containing solutions (at h and i) revealed a small component of trans-activated  $\text{Na}^+$  efflux that was not mediated by the pump (ouabain was still present), and a somewhat enhanced non-TTX-sensitive conductance.

Using the least-squares fitting procedure described for Fig. 5, the segment of palytoxin-induced flux and current data marked by the red trace in Fig. 6 gave an estimate for  $n'$  of 0.96.

#### Effect of Membrane Potential on the Value of $n'$

By exploiting the action of external  $\text{K}^+$  to close pump-channels and accelerate dissociation of palytoxin, repeated

estimations of  $n'$  could be made for the same population of pump-channels under different conditions. Fig. 7 shows 1 of 11 experiments in which membrane potential was varied, in this case from 0 to  $-20$  mV. Starting with  $\text{K}^+$ -free and  $\text{Na}^+$ -free ( $\text{NMG}^+$ ) external solution, and  $\sim 100$  mM  $\text{Na}^+$ , at 0 mV, the switch to 400 mM  $\text{Na}^+$  (at a) caused the usual small increases in net inward current and  $^{22}\text{Na}^+$  efflux (as in Fig. 6). Activation of electrogenic  $\text{Na}^+/\text{K}^+$  pumping by addition of 20 mM  $\text{K}^+$  (at b) then also elicited the usual increment in  $\text{Na}^+$  efflux accompanied by an outward current shift. Pump inhibition by 100  $\mu\text{M}$  ouabain (at c) in the presence of 20 mM  $\text{K}^+$  caused a reduction of  $\text{Na}^+$  efflux (by 16.4  $\text{pmol cm}^{-2} \text{s}^{-1}$ ) and an inward current shift (of 0.52  $\mu\text{A cm}^{-2}$ ). These specific pump-mediated signals yield an  $F\Delta\Phi_{\text{out}}/\Delta I$  ratio of 3.04, close to the 3.0 expected for stoichiometric 3  $\text{Na}^+ : 2 \text{K}^+$  transport (Rakowski et al., 1989). For similarly treated axons that contributed  $n'$  values included in Table I, ouabain-sensitive  $F\Delta\Phi_{\text{out}}/\Delta I$  ratios averaged  $3.09 \pm 0.13$ ,  $n = 5$ , supporting the identical origins of flux and current signals in all of these experiments.

After switching back to ouabain-free,  $\text{K}^+$ -free, 400 mM  $\text{Na}^+$  solution (at d), temporary exposure to 10 nM palytoxin (e to f) induced somewhat delayed increases in inward current and  $\text{Na}^+$  efflux, despite the previous application of ouabain. This contrasts with the lack of effect of 10 nM palytoxin when applied after ouabain in  $\text{Na}^+$ -free external solution (Fig. 4). The effects of palytoxin were reversed (as in Fig. 6) by readdition of 100  $\mu\text{M}$  ouabain (at g) and switching the extracellular solution to  $\text{Na}^+$ -free 400 mM  $\text{K}^+$  without ouabain (at h). The palytoxin-induced increases in current and efflux were fitted during the period indicated by the red trace, and yielded an estimate for  $n'$  of 1.14.

Following a second exposure to 400 mM  $\text{K}^+$  solution (from j to k) to complete the recovery from palytoxin action (signaled by the return of current and flux levels to near extrapolated baseline values; blue lines), membrane potential was stepped from 0 to  $-20$  mV (at l). This caused a small inward holding current shift but no measurable change in  $\text{Na}^+$  efflux. At  $-20$  mV, brief application of 10 nM palytoxin (from m to n) caused a larger increase in inward current, but smaller increase in  $\text{Na}^+$  efflux, than seen earlier at 0 mV. Nevertheless, the value of  $n'$  estimated from the palytoxin-induced flux and current changes at  $-20$  mV was 1.14, identical to that determined at 0 mV. Switching to  $\text{Na}^+$ -free 400 mM  $\text{K}^+$  solution (o to p) again led to almost complete recovery of  $\text{Na}^+$  efflux and membrane current. Fig. S2 shows an experiment similar to that of Fig. 7 but with four applications of palytoxin, at holding potentials of  $-20$ , 0,  $-40$ , and again 0 mV.

#### Influence of $[\text{Na}^+]_o$ on the Value of $n'$

We used the same protocol, transient exposure to palytoxin with termination of its action by ouabain, and



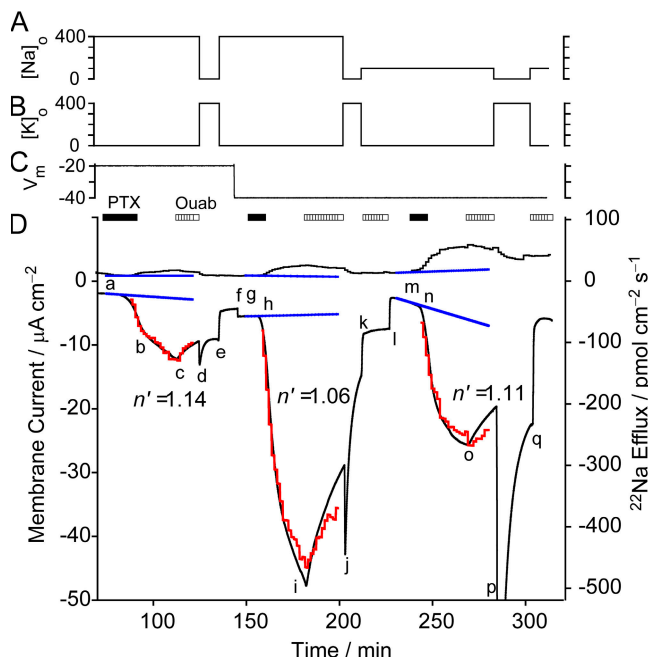


**Figure 8.** External  $\text{Na}^+$  concentration does not alter the flux ratio exponent  $n'$ . The axon was internally dialyzed with 99 mM  $\text{Na}^+$  and subjected to three applications of palytoxin, two at 400 mM and one at 100 mM external  $[\text{Na}^+]_o$ . (A and B)  $\text{Na}^+$  and  $\text{K}^+$  composition of the superfusate. (C) Membrane potential. (D)  $^{22}\text{Na}^+$  efflux and net membrane current. Top bars mark palytoxin treatments (solid bars; 5 nM) and ouabain exposures (hatched bars; 100  $\mu\text{M}$ ). The sequence of changes in the external solution composition is similar to that described for the experiment in Fig. 7. Blue and red lines have the same meaning as in previous figures.

recovery speeded by external  $\text{K}^+$ , to examine the influence of  $[\text{Na}^+]_o$  on the flux-ratio exponent  $n'$  of palytoxin-bound pump-channels. In the axon of Fig. 8, with  $\sim 100$  mM  $\text{Na}^+_i$ ,  $n'$  was estimated first in 400 mM  $\text{Na}^+_o$  at a holding potential of  $-20$  mV, then in 400 mM  $\text{Na}^+_o$  at  $-40$  mV, and finally in 100 mM  $\text{Na}^+_o$  at  $-40$  mV, yielding values for  $n'$  of 1.14, 1.06, and 1.11, respectively.

Table I summarizes estimates for  $n'$  under various experimental conditions. In all cases  $n'$  was close to 1.0, and the values from the different conditions did not differ significantly from each other. We could detect no dependence of  $n'$  on either membrane potential or  $\text{Na}^+_o$ . Statistically, the overall average value of  $n'$  ( $1.05 \pm 0.02$ ,  $n = 28$ ), and the average for 400 mM  $\text{Na}^+_o$  at 0 mV ( $1.07 \pm 0.02$ ,  $n = 13$ ), both differ significantly from 1.0 ( $P < 0.01$ ). But the difference is small (5–7%) and could reflect systematic experimental error.

#### Withdrawal of ATP

Consistent with findings on mammalian  $\text{Na}^+/\text{K}^+$  pumps, in which withdrawal of ATP decreased the apparent affinity for palytoxin action (Artigas and Gadsby, 2004) and lowered the open probability of palytoxin-bound pump-channels (Artigas and Gadsby, 2003a), palytoxin action on  $\text{Na}^+/\text{K}^+$  pumps in squid axons dialyzed with

TABLE I

Mean Value of $n'$ for Various Experimental Conditions		
Experimental Condition	Mean $n' \pm \text{SEM}$	No. of Meas.
400 mM $[\text{Na}]_o / 100$ mM $[\text{Na}]_i$		
0 mV	$1.07 \pm 0.02^a$	13
$-20$ mV	$1.06 \pm 0.04$	5
$-40$ mV	$1.02 \pm 0.04$	6
100 mM $[\text{Na}]_o / 100$ mM $[\text{Na}]_i$		
$-40$ mV	$1.04 \pm 0.06$	4
All data combined	$1.05 \pm 0.02^a$	28

<sup>a</sup>Averages with  $P < 0.01$ .

nucleotide-free solution was slower (Fig. 9, compare with Figs. 5 and 6). The axon in Fig. 9 had been predialyzed with  $\sim 100$  mM  $\text{Na}^+_i$  solution without nucleotides for  $\sim 80$  min before the start of the records illustrated. Addition of 10 mM  $\text{K}^+$  to the  $\text{Na}^+$ -free external solution (a to b) then elicited no measurable  $\text{K}^+_o$ -activated  $\text{Na}^+/\text{K}^+$  pump current or  $^{22}\text{Na}^+$  efflux. However, after switching to  $\text{K}^+$ -free 400 mM  $\text{Na}^+_o$  solution (at c), a high concentration of palytoxin (25 nM; d to e) slowly increased inward current and  $^{22}\text{Na}^+$  efflux, yielding an estimate for  $n'$  of 1.03, indistinguishable from the values obtained in the presence of 5 mM ATP. In the nominal absence of ATP, even low concentrations of external  $\text{K}^+$  (20 mM at f, 50 mM at g) were effective in accelerating closure of palytoxin-bound pump-channels, also in accord with results on mammalian  $\text{Na}^+/\text{K}^+$  pumps (Artigas and Gadsby, 2003a, 2004). Palytoxin caused similar slow increases in current and flux in all three such experiments without ATP.

## DISCUSSION

A voltage-clamped internally dialyzed squid giant axon uniquely allows net current flow across the membrane to be measured simultaneously with unidirectional efflux of a radioactive tracer ion at constant specific activity. Here we exploited that feature to determine the Ussing flux ratio exponent,  $n'$ , for movement of  $\text{Na}^+$  ions through palytoxin-bound  $\text{Na}^+/\text{K}^+$  pump-channels. We first examined palytoxin interactions with native squid axon  $\text{Na}^+/\text{K}^+$  pumps and found that they resemble previously observed interactions with  $\text{Na}^+/\text{K}^+$  pumps from vertebrates. We found the Ussing flux ratio exponent for  $\text{Na}^+$  to be  $\sim 1.0$ , and we found that biionic reversal potentials were invariant over a 10-fold range of permeant ion concentration. Below, we attempt to interpret these findings in terms of  $\text{Na}^+$  ion occupancy and permeation mechanism in palytoxin-bound pump-channels.

#### Interactions of Palytoxin with Na/K Pumps in Squid Neurons and Axons

For technical reasons, we made some measurements in patches excised from giant-fiber lobe neurons of the

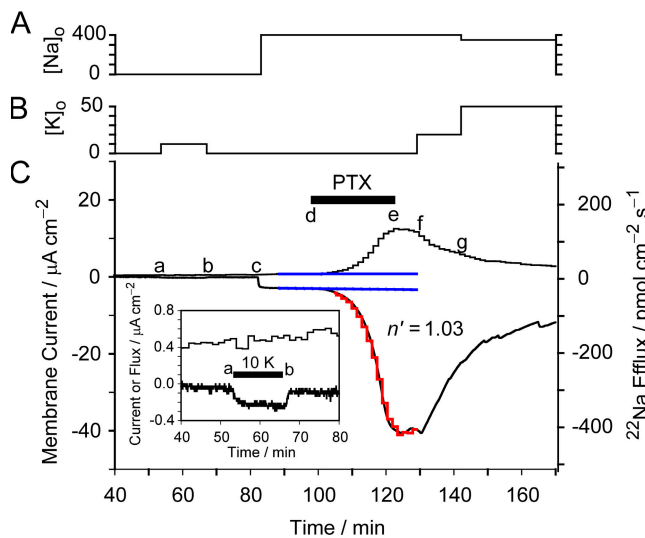


**Figure 9.** Absence of nucleotide does not alter the flux ratio exponent  $n'$ . The axon was internally dialyzed with nucleotide-free, 99 mM  $\text{Na}^+$  solution and held at 0 mV throughout. (A and B)  $\text{Na}^+$  and  $\text{K}^+$  composition of the superfusate. (C)  $^{22}\text{Na}^+$  efflux and net membrane current. The inset amplifies the data for the period between 40 and 80 min, showing the lack of outward electrogenic pump current or associated increase of  $^{22}\text{Na}^+$  efflux after addition of 10 mM  $\text{K}^+$  to the  $\text{Na}^+$ -free external solution. A detailed description of the experiment is given in the text. Blue and red lines have the same meaning as in previous figures.

stellate ganglion and we made others in the giant axons that emanate from those neurons. But available data suggest that a single  $\text{Na}^+/\text{K}^+$  pump  $\alpha$ -subunit (SqNaK  $\alpha 1$ ; Genbank/EMBL/DDBJ no. EF467997) is the major isoform in this contiguous giant axon system (Colina et al., 2007). Messenger RNA for SqNaK  $\alpha 1$  is abundant in the giant-fiber lobe neurons, and all 16  $\text{Na}^+/\text{K}^+$  pump  $\alpha$ -subunit clones isolated from a squid stellate ganglion EST library were homologous to the SqNaK  $\alpha 1$  sequence. Moreover, PCR reactions using degenerate primers exclusively amplified this sequence (Colina et al., 2007).

The estimated  $K_{0.5}$  of  $\sim 70$  pM (Fig. 2 D) for palytoxin activation of current in outside-out patches from giant fiber lobe neurons, with internal and external solutions containing high  $[\text{Na}^+]$  (but no  $\text{K}^+$ ), is similar to the  $K_{0.5}$  of  $\sim 30$  pM found for  $\text{Na}^+/\text{K}^+$  pumps in HEK293 cells under comparable (other than ionic strength) conditions (Artigas and Gadsby, 2004). Also similar to findings on  $\text{Na}^+/\text{K}^+$  pumps in mammalian cells (Artigas and Gadsby, 2003a, 2004), replacing external  $\text{Na}^+$  with  $\text{K}^+$  accelerated palytoxin unbinding from pumps in squid axons (Figs. 6–9). Acceleration of the decay of current and  $^{22}\text{Na}$  efflux by external  $\text{K}^+$  can be interpreted as  $\text{K}^+$ -induced closure of the  $\text{Na}^+/\text{K}^+$  pump's external gate, with occupation of the ion-binding sites by occluded  $\text{K}^+$  ions. Because palytoxin binds most tightly to, and hence stabilizes, a conformation with the extracellular gate open, the action of external  $\text{K}^+$  promotes dissociation

of palytoxin (Artigas and Gadsby, 2004; Harmel and Apell, 2006).

Withdrawal of nucleotides (by internal dialysis), until  $[\text{ATP}]$  in the axon was too low to support measurable  $\text{Na}^+/\text{K}^+$  exchange, did not prevent palytoxin from slowly increasing conductance (Fig. 9). We previously found that even submicromolar  $[\text{ATP}]$  could enhance palytoxin apparent affinity in mammalian  $\text{Na}^+/\text{K}^+$  pumps, probably by supporting pump phosphorylation (Artigas and Gadsby, 2003b, 2004). Nevertheless, at such low  $[\text{ATP}]$ , the apparent affinity for palytoxin binding and the open probability of palytoxin-bound  $\text{Na}^+/\text{K}^+$  pump-channels were both lower than at millimolar  $[\text{ATP}]$  levels (Artigas and Gadsby, 2003a). Similarly lowered palytoxin affinity, and open probability of pump-channels, after dialyzing intra-axonal  $[\text{ATP}]$  down to submicromolar levels, can explain the relatively slow response to palytoxin in Fig. 9.

Two of our findings in squid axons demonstrate that palytoxin and ouabain can both simultaneously occupy the same pump molecule, as established for mammalian  $\text{Na}^+/\text{K}^+$  pumps (Artigas and Gadsby, 2004). First, squid  $\text{Na}^+/\text{K}^+$  pumps are inhibited, practically irreversibly, by submicromolar ouabain concentrations (Baker et al., 1969), and yet after addition of 100  $\mu\text{M}$  ouabain, enough to inhibit every pump in the axon (Fig. 7 c), palytoxin still readily transformed  $\text{Na}^+/\text{K}^+$  pumps into channels (Fig. 7, e and m). Palytoxin must therefore have interacted with squid  $\text{Na}^+/\text{K}^+$  pumps to which ouabain was already bound. Second, addition of 100  $\mu\text{M}$  ouabain, shortly after withdrawal of palytoxin, promptly diminished the net current and  $^{22}\text{Na}$  efflux flowing through palytoxin-bound  $\text{Na}^+/\text{K}^+$  pump-channels (Fig. 7 g; Fig. 8, c, i, and o; Fig. S2, c, i, o, and u). Because in all cases palytoxin-induced current and efflux were still growing at the time of ouabain addition, ouabain must have acted on palytoxin-bound pump-channels. The slower time courses of palytoxin-induced current and efflux increase observed when palytoxin was applied after ouabain (Figs. 7, 8, and S2), rather than before ouabain (Figs. 5 and 6), support the proposal that ouabain unbinding from the palytoxin-ouabain pump complex is the rate-limiting step for pump-channel opening (Artigas and Gadsby, 2004). Because ouabain would remain tightly bound to the  $\text{Na}^+/\text{K}^+$  pump in the absence of palytoxin, these results also further demonstrate that palytoxin binds to and destabilizes the ouabain pump complex, and that ouabain keeps palytoxin-bound pump-channels closed (Artigas and Gadsby, 2004).

#### Permeation Characteristics of Palytoxin-opened Channels in Squid Na/K Pumps

The single-channel conductance of palytoxin-opened channels in squid  $\text{Na}^+/\text{K}^+$  pumps,  $\sim 7$  pS in  $\sim 500$  mM  $[\text{Na}^+]$  solutions (Fig. 2), is similar to that of  $\sim 8$  pS for pump-channels in HEK cells,  $\sim 7$  pS in cardiac myocytes,

and  $\sim 5$  pS in *Xenopus* oocytes, in all cases in  $\sim 150$  mM  $[\text{Na}^+]$  solutions (Artigas and Gadsby, 2004, 2006). Comparable values, 7–10 pS, were reported previously for palytoxin-bound pump-channels in a variety of preparations (e.g., Ikeda et al., 1988; Muramatsu et al., 1988; Hirsh and Wu, 1997; Wang and Horisberger, 1997). The similar conductances of palytoxin-opened channels in squid and in vertebrates, even though the former were measured at three to four times higher ionic strength, support the suggestion (Colina et al., 2007) that evolution has tuned the electrostatic environment near the external mouth of each pump's permeation pathway to adapt its function to the ionic strength of the prevailing extracellular milieu. In addition, the palytoxin-bound pump-channels of both HEK cells and squid neurons show a small but measurable permeability to  $\text{NMG}^+$ , with  $P_{\text{NMG}}/P_{\text{Na}}$  being 0.024 in squid (Fig. 2 C) and 0.021 in HEK pump-channels, and both are more permeable to  $\text{TMA}^+$  than to  $\text{NMG}^+$ , with  $P_{\text{TMA}}/P_{\text{Na}}$  being 0.10 in squid (Fig. 3) and  $0.16 \pm 0.02$  ( $n = 5$ ) in HEK pump-channels (Artigas and Gadsby, 2004).

Although  $\text{NMG}^+$  ions evidently permeate palytoxin-bound pump-channels, if slowly, external  $\text{NMG}^+$  ions appear to partly block  $\text{Na}^+$  efflux through them. Thus, at large positive membrane potentials ( $>50$  mV), outward  $\text{Na}^+$  current through pump-channels in outside-out patches was immediately reduced almost twofold (Fig. 2, A–C) by suddenly replacing 460 mM external  $\text{Na}^+$  with 460 mM external  $\text{NMG}^+$  (see Fig. 1 legend in Artigas and Gadsby, 2004). A further indication of block by external  $\text{NMG}^+$  is that palytoxin-induced  $^{22}\text{Na}$  efflux was smaller in axons bathed in 400 mM  $\text{NMG}^+$  (Fig. 4) than in axons bathed in 400 mM  $\text{Na}^+$  (e.g., Figs. 5, 6), despite their identical 100 mM internal  $[\text{Na}^+]$ ; nonindependence of  $\text{Na}^+$  movements (see below) would be expected to have the opposite effect, diminishing  $^{22}\text{Na}$  efflux in the presence of external  $\text{Na}^+$ . A reduction of the apparent affinity for palytoxin in the absence of external  $\text{Na}^+$  could possibly contribute to this smaller palytoxin response in external  $\text{NMG}^+$ , but it could not account for the near-instantaneous blocking action of  $\text{NMG}^+$  (Fig. 2, A–C); that block is rapidly relieved on switching back to  $\text{Na}^+$  solution even after washout of unbound palytoxin (e.g., Artigas and Gadsby, 2004, 2006).

#### $\text{Na}^+$ Ion Occupancy and Permeation in Palytoxin-bound Pump-Channels

Measurable permeation of pump-channels by  $\text{NMG}^+$ , in both squid neurons (Fig. 2) and HEK cells (Artigas and Gadsby, 2004), indicates that the narrowest region of their pore must be  $\sim 7.5$  Å wide. This raises the question of whether  $\text{Na}^+$  ions can pass each other in these channels and perhaps move independently of one another, or whether instead they are constrained to move in single file and, if so, whether the open channel

contains a queue of several  $\text{Na}^+$  ions, or just one  $\text{Na}^+$  ion at a time. To address these questions we took two different approaches.

The first established that the reversal potentials of palytoxin-induced currents under similar biionic conditions, i.e., with equal concentrations of internal  $\text{Na}^+$  and external  $\text{TMA}^+$  as the permeant ions, were independent of those concentrations over a 10-fold range, from 55 to 550 mM (Fig. 3). The ratio of the permeabilities of these two ions, at least as defined for Nernst-Planck electrodiffusion (e.g., Hille and Schwarz, 1978), must therefore also be independent of concentration.

The second approach used simultaneous measurements of palytoxin-induced net current and unidirectional  $^{22}\text{Na}$  efflux to calculate corresponding unidirectional  $\text{Na}^+$  influx, and hence the Ussing flux ratio exponent,  $n'$ . These estimates depend on the accuracy of the simultaneous current and flux measurements as well as on the validity of the assumption that they derive from the same area of axon membrane, i.e., from the axon segment in the central superfusion pool that is isolated electrically by auxiliary voltage-clamp circuitry and mechanically by narrow grease seals (Rakowski, 1989; Rakowski et al., 1989). We previously demonstrated that all these requirements are met by showing that, in  $\text{Na}^+_{\text{o}}$ -free solution, TTX-induced decrements of  $^{22}\text{Na}$  efflux and of net outward current are equivalent (Rakowski et al., 1989, 2002); we have repeated that demonstration here (Fig. S1). We also established, for several of the axons used here to obtain  $n'$  values of palytoxin-bound pump-channels, that ouabain-sensitive,  $\text{Na}^+/\text{K}^+$  pump-mediated  $^{22}\text{Na}$  efflux and net outward current displayed the ratio (equivalent to 3.0) appropriate for stoichiometric  $3 \text{Na}^+ : 2 \text{K}^+$  transport (Rakowski et al., 1989); and we obtained the same stoichiometry for  $\text{K}^+_{\text{o}}$  activation of the pump in  $\text{Na}^+_{\text{o}}$ -free solution, in the experiment of Fig. 4 (a to b). These results validate the comparisons of fluxes and currents presented here. Hence, the finding that, with  $\text{Na}^+_{\text{o}}$ -free solution, palytoxin elicited equivalent increments in  $^{22}\text{Na}$  efflux and in outward current (Fig. 4, c to d) allowed the further conclusion that  $\text{Na}^+$  ions were the principal current carriers through pump-channels during the present experiments designed to estimate flux ratios (Figs. 5–9). Mean values of  $n'$  were determined for 100 mM  $\text{Na}^+_{\text{i}}$ , with 400 mM  $\text{Na}^+_{\text{o}}$  at 0,  $-20$ , and  $-40$  mV, and with 100 mM  $\text{Na}^+_{\text{o}}$  at  $-40$  mV (Table I). They included estimates in the nominal absence of ATP, they were all close to 1.0, and they were not statistically significantly different from each other or from the overall average, which was  $1.05 \pm 0.02$  ( $n = 28$ ), barely statistically significantly different from 1.0 ( $P < 0.01$ ).

Our findings with the two approaches, i.e., the independence of biionic reversal potential from ion concentration and a flux ratio exponent of 1.0, could be explained by any of several possibilities ranging from the very general to the highly constrained. Thus, pump-channels

(a) could allow free diffusion of  $\text{Na}^+$  ions and obey the independence principle (Hodgkin and Huxley, 1952), or (b) they could contain a single  $\text{Na}^+$  ion-binding site, or (c) they could be multisite channels that do not show single-filing, or (d) multisite single-file channels that rarely contain more than one ion at a time (e.g., Lauger, 1973; Hille and Schwarz, 1978; Levitt, 1986; Zarei and Dani 1994; Hille, 2001), or (e) they could be multiply occupied single-file channels with permeation characteristics that meet certain specific constraints (Kohler and Heckmann, 1979; Schumaker and MacKinnon, 1990).

The first possibility can be ruled out because the conductance of single palytoxin-bound pump-channels was found to be a saturable function of  $\text{Na}^+$  activity (Artigas and Gadsby, 2006), which means that  $\text{Na}^+$  movements through these channels do not obey independence; at high  $[\text{Na}^+]$  activity, interactions of  $\text{Na}^+$  ions with pump-channels become influenced by  $\text{Na}^+$  ions already in the pores (e.g., Hille, 2001). The relatively low apparent affinity of the putative  $\text{Na}^+$  binding site(s) associated with this saturable behavior ( $K_{0.5} \sim 300 \text{ mM } [\text{Na}^+]$  for pump-channels in *Xenopus* oocytes; Artigas and Gadsby, 2006) is consistent with the fluxes of millions of  $\text{Na}^+$  ions per second observed to flow through palytoxin-bound pump-channels (e.g., Fig. 1), under which conditions each  $\text{Na}^+$  ion must spend  $< 1 \mu\text{s}$  inside an open channel.

Distinguishing between the remaining possibilities is difficult. Our results are all consistent with pump-channels being occupied by only a single ion, whether they contain a single binding site, or more than one binding site without, or with, single filing. However,  $\text{Na}^+/\text{K}^+$  pumps are known to contain multiple ion-binding sites, and crystal structures of  $\text{Ca}^{2+}$ -bound sarcoplasmic and endoplasmic reticular  $\text{Ca}^{2+}$  pumps, homologues of  $\text{Na}^+/\text{K}^+$  pump  $\alpha$  subunits, all show that they are occupied by two  $\text{Ca}^{2+}$  ions. The ions lie deep inside the protein, nearly halfway across the membrane, but they are arranged side by side rather than in single file (Toyoshima et al., 2000, 2004; Sørensen et al., 2004; Toyoshima and Mizutani, 2004). Not surprisingly, models of the  $\text{Na}^+/\text{K}^+$  pump  $\alpha$ -subunit based on those crystal structures picture similar side-by-side binding sites for three  $\text{Na}^+$  ions in E1-like conformations (Ogawa and Toyoshima 2002; Rakowski and Sagar, 2003), or for two  $\text{K}^+$  ions in E2-like conformations (Ogawa and Toyoshima 2002). Negative charges of conserved acidic side chains are expected to help coordinate the  $\text{Na}^+$  or  $\text{K}^+$  ions in these ion-binding sites in  $\text{Na}^+/\text{K}^+$  pumps (Nielsen et al., 1998; Ogawa and Toyoshima 2002; Toyoshima and Nomura, 2002; Toyoshima et al., 2004; Møller et al., 2005). Indeed, side chains of residues in at least two of the positions that contribute to one of those ion-binding sites (site II, between the fourth and sixth transmembrane helices) are accessible from the ion pathway within palytoxin-bound pump-channels (Reyes and Gadsby 2006), arguing that  $\text{Na}^+$  ions flowing through them

traverse, and hence at least transiently occupy, site II. But occupancy of more than one site by  $\text{Na}^+$  may be anticipated in palytoxin-bound pump-channels, because palytoxin is believed to stabilize an E2P-like conformation of the  $\text{Na}^+/\text{K}^+$  pump (Artigas and Gadsby, 2004; Harmel and Apell, 2006; Reyes and Gadsby 2006), a conformation that in the absence of palytoxin binds two  $\text{K}^+$  ions (e.g., Glynn and Karlish, 1990) or two  $\text{Na}^+$  ions (e.g., Sturmer and Apell, 1992). Moreover, fluorescence levels of electrochromic styryl reporter dyes indicate occupancy of palytoxin-bound pump-channels by either two  $\text{Na}^+$  ions, two  $\text{K}^+$  ions, or two protons (Harmel and Apell, 2006). An intriguing possibility, then, is that in the present experiments palytoxin-bound pump-channels are also mostly occupied by two  $\text{Na}^+$  ions, but that they reside side by side, in sites I and II, rather than in single file. If only the site II ion has ready access to both sides of the membrane in the palytoxin-stabilized pump conformation, this could explain the observed behavior resembling that of a pore that is rarely occupied by more than one ion.

We note that, in contrast to this side-by-side architecture expected for ion-binding sites in  $\text{Na}^+/\text{K}^+$  pumps, ion-binding sites in voltage-gated  $\text{Na}^+$  channels may be expected to align in single file (due to structural homology of their ion pore to that of  $\text{K}^+$  channels; Doyle et al., 1998). In squid axons, voltage-gated  $\text{Na}^+$  channels do display characteristics of single-file pores with two ion-binding sites (Begenisich and Cahalan, 1980), but, like palytoxin-bound  $\text{Na}^+/\text{K}^+$  pumps, they exhibit an Ussing flux ratio exponent close to 1.0 (Begenisich and Busath, 1981; Rakowski et al., 2002); given their low apparent affinity for  $\text{Na}^+$ , the preferred interpretation is that voltage-gated  $\text{Na}^+$  channels are single-file multisite pores that are seldom occupied by more than one ion at a time. Although it remains formally possible that palytoxin-bound  $\text{Na}^+/\text{K}^+$  pump-channels are also single-file multisite pores with single ion occupancy, as noted above structural considerations and fluorescence data argue for occupancy by two ions. However, provided that certain kinetic constraints apply, the invariance of the biionic reversal potential and the flux ratio exponent close to 1.0 could also both be explained if pump-channels were single-file pores containing two  $\text{Na}^+$  ion-binding sites that are mostly occupied. The necessary constraints are that (a) the channels operate by a single-vacancy flux mechanism (which requires that rates of ion hopping between sites exceed ion exit rates), and furthermore, (b) in the biionic experiments, the ratio of the exit rates for the two ions approximate the square of the ratio of their hopping rates, and (c) in the flux ratio measurements, the rate of entry of  $\text{Na}^+$  ions into the pump-channels substantially exceeds their hopping rate (Kohler and Heckmann, 1979; Schumaker and MacKinnon, 1990). This specific combination of constraints seems idiosyncratic, but we know too little about the permeation properties of palytoxin-bound pump-channels to rule any of them out with any confidence.

Overall, in view of structural evidence for multiple side-by-side rather than single-file binding sites in this family of ion pumps, for expected occupancy of more than one site in palytoxin-bound Na<sup>+</sup>/K<sup>+</sup> pump-channels, and yet for ready accessibility of only one of those sites, we postulate that pump-channels are nearly always occupied by two Na<sup>+</sup> ions, side by side, but that their readily accessible ion pathway rarely contains more than a single Na<sup>+</sup> ion, so accounting for their Ussing flux ratio exponent of ~1.0. Different kinds of measurements will be required to test this hypothesis.

We thank Mr. Chandrakanth Reddy for computational assistance and Mark Mayer (National Institutes of Health [NIH], Bethesda, MD) for the donation of electrophysiological equipment.

This work was supported by NIH grants NS22979, NS11223, and HL36783, and National Science Foundation grant CCF-0622158. This research was also partially funded by the Intramural Research Program of the NIH, National Institute of Neurological Disorders and Stroke.

Ted Begenisich served as guest editor.

Submitted: 1 March 2007

Accepted: 22 May 2007

## REFERENCES

- Artigas, P., and D.C. Gadsby. 2003a. Na<sup>+</sup>/K<sup>+</sup>-pump ligands modulate gating of palytoxin-induced ion channels. *Proc. Natl. Acad. Sci. USA*. 100:501–505.
- Artigas, P., and D.C. Gadsby. 2003b. Ion occlusion/deocclusion partial reactions in individual palytoxin-modified Na/K pumps. *Ann. N. Y. Acad. Sci.* 986:116–126.
- Artigas, P., and D.C. Gadsby. 2004. Large diameter of palytoxin-induced Na/K pump-channels and modulation of palytoxin interaction by Na/K pump ligands. *J. Gen. Physiol.* 123:357–376.
- Artigas, P., and D.C. Gadsby. 2006. Ouabain affinity determining residues lie close to the Na/K pump ion pathway. *Proc. Natl. Acad. Sci. USA*. 103:12613–12618.
- Baker, P.F., M.P. Blaustein, R.D. Keynes, J. Manil, T.I. Shaw, and R.A. Steinhardt. 1969. The ouabain-sensitive fluxes of sodium and potassium in squid giant axons. *J. Physiol.* 200:459–496.
- Begenisich, T., and D. Busath. 1981. Sodium flux ratio in voltage-clamped squid giant axons. *J. Gen. Physiol.* 77:489–502.
- Begenisich, T., and M.D. Cahalan. 1980. Sodium channel permeation in squid axons. I: Reversal potential experiments. *J. Physiol.* 307:217–242.
- Colina, C., J.J.C. Rosenthal, J.A. DeGiorgis, D. Srikumar, N. Iruku, and M. Holmgren. 2007. Structural basis of Na<sup>+</sup>/K<sup>+</sup>-ATPase adaptation to marine environments. *Nat. Struct. Mol. Biol.* 14:427–431.
- Doyle, D.A., J. Morais Cabral, R.A. Pfuetzner, A. Kuo, J.M. Gulbis, S.L. Cohen, B.T. Chait, and R. MacKinnon. 1998. The structure of the potassium channel: molecular basis of K<sup>+</sup> conduction and selectivity. *Science*. 280:69–77.
- Gadsby, D.C., R.F. Rakowski, and P. De Weer. 1993. Extracellular access to the Na,K pump: pathway similar to ion channel. *Science*. 260:100–103.
- Gilly, W.F., M.T. Lucero, and F.T. Horrigan. 1990. Control of the spatial distribution of sodium channels in giant fiber lobe neurons of the squid. *Neuron*. 5:663–674.
- Glynn, I.M., and S.J. Karlish. 1990. Occluded cations in active transport. *Annu. Rev. Biochem.* 59:171–205.
- Habermann, E. 1989. Palytoxin acts through Na<sup>+</sup>, K<sup>+</sup>-ATPase. *Toxicol.* 27:1171–1197.
- Hamill, O.P., A. Marty, E. Neher, B. Sakmann, and F.J. Sigworth. 1981. Improved patch-clamp techniques for high-resolution current recording from cells and cell-free membrane patches. *Pflügers Arch.* 391:85–100.
- Harmel, N., and H.-J. Apell. 2006. Palytoxin-induced effects on partial reactions of the Na,K-ATPase. *J. Gen. Physiol.* 128:103–118.
- Hille, B. 2001. Ion Channels of Excitable Membranes. Third edition. Sinauer Associates, Sunderland, MA. 814 pp.
- Hille, B., and W. Schwarz. 1978. Potassium channels as multi-ion single-file pores. *J. Gen. Physiol.* 72:409–442.
- Hirsh, J.K., and C.H. Wu. 1997. Palytoxin-induced single channel currents from the sodium pump synthesized by *in vitro* expression. *Toxicol.* 35:169–176.
- Hodgkin, A.L., and A.F. Huxley. 1952. Currents carried by sodium and potassium through the membrane of the giant axon of *Loligo*. *J. Physiol.* 116:449–472.
- Hodgkin, A.L., and R.D. Keynes. 1955. The potassium permeability of a giant nerve fibre. *J. Physiol.* 128:61–88.
- Horisberger, J.-D. 2004. Recent insights into the structure and mechanism of the sodium pump. *Physiology (Bethesda)*. 19:377–387.
- Ikeda, M., K. Mitani, and K. Ito. 1988. Palytoxin induces a non-selective cation channel in single ventricular cells of rat. *Naunyn-Schmiedeberg Arch. Pharmacol.* 337:591–593.
- Kohler, H.H., and K. Heckmann. 1979. Unidirectional fluxes in saturated single-file pores of biological and artificial membranes. I. Pores containing no more than one vacancy. *J. Theor. Biol.* 79:381–401.
- Läuger, P. 1973. Ion transport through pores: a rate-theory analysis. *Biochim. Biophys. Acta.* 311:423–441.
- Levit, D.G. 1986. Interpretation of biological ion channel flux data: reaction-rate versus continuum theory. *Annu. Rev. Biophys. Biophys. Chem.* 15:29–57.
- Llano, I., and R.J. Bookman. 1986. Ionic conductances of squid giant fiber lobe neurons. *J. Gen. Physiol.* 88:543–569.
- Møller, J.V., P. Nissen, T.L. Sorensen, and M. Maire. 2005. Transport mechanism of the sarcoplasmic reticulum Ca<sup>2+</sup>-ATPase pump. *Curr. Opin. Struct. Biol.* 15:387–393.
- Muramatsu, I., M. Nishio, S. Kigoshi, and D. Uemura. 1988. Single ionic channels induced by palytoxin in guinea pig ventricular myocytes. *Br. J. Pharmacol.* 93:811–816.
- Muramatsu, I., D. Uemura, M. Fujiwara, and T. Narahashi. 1984. Characteristics of palytoxin-induced depolarization in squid axons. *J. Pharmacol. Exp. Ther.* 231:488–494.
- Nielsen, J.M., P.A. Pedersen, S.J. Karlish, and P.L. Jorgensen. 1998. Importance of intramembrane carboxylic acids for occlusion of K<sup>+</sup> ions at equilibrium in renal Na,K-ATPase. *Biochemistry*. 37:1961–1968.
- Ogawa, H., and C. Toyoshima. 2002. Homology modeling of the cation binding sites of Na<sup>+</sup>, K<sup>+</sup>-ATPase. *Proc. Natl. Acad. Sci. USA*. 99:15977–15982.
- Pedersen, P.A., J.M. Nielsen, J.H. Rasmussen, and P.L. Jorgensen. 1998. Contribution to Tl<sup>+</sup>, K<sup>+</sup>, and Na<sup>+</sup> binding of Asn776, Ser775, Thr774, Thr772, and Tyr771 in cytoplasmic part of fifth transmembrane segment in  $\alpha$ -subunit of renal Na,K-ATPase. *Biochemistry*. 37:17818–17827.
- Pichon, Y. 1982. Effects of palytoxin on sodium and potassium permeabilities in unmyelinated axons. *Toxicol.* 20:41–47.
- Rakowski, R.F. 1989. Simultaneous measurement of changes in current and tracer flux in voltage-clamped squid giant axon. *Biophys. J.* 55:663–671.
- Rakowski, R.F., D.C. Gadsby, and P. De Weer. 1989. Stoichiometry and voltage dependence of the sodium pump in voltage-clamped, internally dialyzed squid giant axon. *J. Gen. Physiol.* 93:903–941.
- Rakowski, R.F., D.C. Gadsby, and P. De Weer. 2002. Single sodium ion occupancy and steady state gating of the tetrodotoxin sensitive channels in squid giant axon. *J. Gen. Physiol.* 119:235–249.

- Rakowski, R.F., and S. Sagar. 2003. Found: Na<sup>+</sup> and K<sup>+</sup> binding sites of the sodium pump. *News Physiol. Sci.* 18:164–168.
- Reyes, N., and D.C. Gadsby. 2006. Ion permeation through the Na<sup>+</sup>,K<sup>+</sup>-ATPase. *Nature.* 443:470–474.
- Rouzaire-Dubois, B., and J.M. Dubois. 1990. Characterization of palytoxin-induced channels in mouse neuroblastoma cells. *Toxicol.* 28:1147–1158.
- Scheiner-Bobis, G., D. Meyer zu Heringdorf, M. Christ, and E. Habermann. 1994. Palytoxin induces K<sup>+</sup> efflux from yeast cells expressing the mammalian sodium pump. *Mol. Pharmacol.* 45:1132–1136.
- Schumaker, M.F., and R. MacKinnon. 1990. A simple model for multi-ion permeation. Single-vacancy conduction in a simple pore model. *Biophys. J.* 58:975–984.
- Sørensen, T.L.-M., J.V. Møller, and P. Nissen. 2004. Phosphoryl transfer and calcium ion occlusion in the calcium pump. *Science.* 304:1672–1675.
- Sturmer, W., and H.-J. Apell. 1992. Fluorescence study on cardiac glycoside binding to the Na,K-pump. Ouabain binding is associated with movement of electrical charge. *FEBS Lett.* 300:1–4.
- Tosteson, M.T., J.A. Halperin, Y. Kishi, and D.C. Tosteson. 1991. Palytoxin induces an increase in the cation conductance of red cells. *J. Gen. Physiol.* 98:969–985.
- Tosteson, M.T. 2000. Mechanism of action, pharmacology and toxicology. In *Seafood and Freshwater Toxins Pharmacology, Physiology, and Detection*. L.M. Botana, editor. Marcel Dekker, New York. 549–566.
- Toyoshima, C., and T. Mizutani. 2004. Crystal structure of the calcium pump with a bound ATP analogue. *Nature.* 430:529–535.
- Toyoshima, C., M. Nakasako, H. Nomura, and H. Ogawa. 2000. Crystal structure of the calcium pump of sarcoplasmic reticulum at 2.6 Å resolution. *Nature.* 405:647–655.
- Toyoshima, C., and H. Nomura. 2002. Structural changes in the calcium pump accompanying the dissociation of calcium. *Nature.* 418:605–611.
- Toyoshima, C., H. Nombra, and T. Tsuda. 2004. Luminal gating mechanism revealed in calcium pump crystal structures with phosphate analogues. *Nature.* 432:361–368.
- Ussing, H.H. 1949. The distinction by means of tracers between active transport and diffusion. The transfer of iodide across the isolated frog skin. *Acta Physiol. Scand.* 19:43–56.
- Wang, X., and J.-D. Horisberger. 1997. Palytoxin effect through interaction with the Na,K-ATPase in *Xenopus* oocytes. *FEBS Lett.* 409:391–395.
- Zarei, M., and J.A.X. Dani. 1994. Ionic permeability characteristics of the N-methyl-D-aspartate receptor channel. *J. Gen. Physiol.* 103:231–248.